Table S1: Sampling periods of KH-13-7 cruise.

No.	Start time (UTC) End time (UTC)	Start point End point	Total Flow (m^3)
13-a	12 Dec, 11:04 p.m. 15 Dec, 10:00 p.m.	29.22º N, 147.92º E 20.00º N, 160.00º E	923.14
13-b	15 Dec, 10:05 p.m. 18 Dec, 9:01 p.m.	20.00º N, 160.00º E 11.80º N, 172.28º E	717.09
13-c	2 Feb, 10:12 p.m. 5 Feb, 11:05 p.m.	3.67º N, 159.44º E 19.39º N, 150.31º E	734.02
13-d	5 Feb, 11:08 p.m. 9 Feb, 0:03 a.m.	19.39º N, 150.31º E 29.62º N, 142.33º E	605.99
13-e	9 Feb, 0:05 a.m. 11 Feb, 0:03 a.m.	29.62º N, 142.33º E 35.17º N, 139.77º E	597.42

Table S2. Sampling periods of KH-14-3 cruise.

No.	Start time (UTC) End time (UTC)	Start point End point	Total Flow (m^3)
14-A	24 June, 0:13 a.m. 26 June, 10:04 p.m.	32.40º N, 143.09º E 22.00º N, 157.26º E	710.64
14-B	26 June, 10:06 a.m. 28 June, 1:08 p.m.	22.00º N, 157.26º E 17.56º N, 163.05º E	468.72
14-C	30 June, 10:04 p.m. 3 July, 8:00 p.m.	10.33º N, 174.18º E 1.24º N, 171.45º W	887.42
14-D	3 July, 8:04 p.m. 6 July, 7:55 p.m.	1.24º N, 171.45º W 10.02º N, 170.02º W	818.32
14-E	6 July, 7:57 p.m. 9 July, 8:20 p.m.	10.02º N, 170.02º W 20.01º N, 169.57º W	864.71
14-F	9 July, 8:22 p.m. 12 July, 6:59 p.m.	20.01º N, 169.57º W 20.46º N, 161.33º W	871.97
14-G	12 July, 7:02 p.m. 13 July, 3:57 p.m.	20.46º N, 161.33º W 21.01º N, 157.59º W	228.41
14-H	18 July, 4:13 a.m. 20 July, 8:01 p.m.	21.51º N, 157.36º W 30.02º N, 170.01º W	345.16
14-I	20 July, 8:03 p.m. 23 July, 7:58 p.m.	30.02º N, 170.01º W 40.03º N, 171.00º W	898.01
14-J	23 July, 8:00 p.m. 26 July, 8:00 p.m.	40.03º N, 171.00º W 50.02º N, 169.56º W	933.27
14-K	26 July, 8:02 p.m. 29 July, 8:57 p.m.	50.02º N, 169.56º W 63.38º N, 167.38º W	944.25
14-L	29 July, 9:01 p.m. 1 Aug, 8:59 p.m.	63.38º N, 167.38º W 60.44º N, 176.03º W	748.4
14-M	1 Aug, 9:00 p.m. 1 Aug, 9:57 p.m.	60.44º N, 176.03º W 47.39º N, 167.08º E	954.26
14-N	4 Aug, 10:00 p.m. 8 Aug, 0:05 a.m.	47.39º N, 167.08º E 37.33º N, 145.15º E	926.04
14-O	8 Aug, 0:07 a.m. 8 Aug, 11:59 p.m.	37.33º N, 145.15º E 35.26º N, 139.48º E	293.43

Table S3. The flow of Fe separation with the anion exchange resin.

	Objective	**Solution**	**Volume per each introduction [µL]**	**Repetition**
1.	Rinse	6 M HCl	250	4
2.	Rinse	UPW	60	5
3.	Conditioning	6 M HCl/0.3 mM H_2O_2	200	1
4.	Sample introduction	Sample in 6 M HCl/0.3 mM H_2O_2	200	1
5.	Elution of Cu, Cr	6 M HCl/0.3 mM H_2O_2	30	14
6.	Elution of Fe	1 M HCl/0.3 mM H_2O_2	30	12

Table S4. Atmospheric Fe concentrations and isotope ratios of total (acid-digested) and soluble Fe of the KH-13-7 samples. n.a.: not available due to small quantity of sample Fe or high filter blank.

No.	Coarse			Fine			Bulk (Coarse+Fine)
	Fe conc. ($ng\ m^{-3}$) *	δ^{56}Fe±2SE (‰) **		Fe conc. ($ng\ m^{-3}$) **	δ^{56}Fe ± 2SE (‰) **		δ^{56}Fe ± 2SE (‰)
		Total	Soluble		Total	Soluble	
13-a	8.07 (0.1 %)*	−0.06±0.14 (−0.11±0.13)**	n.a.	4.70 (4 %)	−1.46±0.22 (−1.34±0.21)	n.a.	−0.58±0.12
13-b	0.47 (2 %)	0.10±0.25 (0.09±0.24)	n.a.	0.54 (29 %)	−0.01±0.23 (0.02±0.22)	n.a.	0.04±0.17
13-c	1.28 (1 %)	0.38±0.28 (0.38±0.26)	n.a.	0.77 (22 %)	0.15±0.20 (0.02±0.22)	n.a.	0.30±0.19
13-d	14.64 (0.1 %)	0.03±0.18 (0.02±0.16)	n.a.	4.15 (6 %)	−0.45±0.28 (−0.42±0.27)	−2.23±0.04	−0.07±0.15
13-e	22.72 (0.1 %)	0.10±0.14 (0.08±0.13)	−0.27±0.03	11.09 (2 %)	−0.47±0.18 (−0.46±0.16)	−1.14±0.03	−0.09±0.11

*Fe concentrations were calculated after subtraction of blank concentration. Fraction of Fe in blank filter to sample filter is shown in the parenthesis.

** δ^{56}Fe values before the correction of blank filter is shown in the parenthesis.

Table S5. Atmospheric Fe concentrations and isotope ratios of total (acid-digested) Fe of the KH-14-3 samples. <D.L.: under detection limit (approximately <0.01 ng m^{-3} and <0.2 ng m^{-3} for coarse and fine particles, respectively), n.a.: not available due to small quantity of sample Fe or high filter blank.

No.	Coarse		Fine		Bulk (Coarse+Fine)
	Fe conc. (ng m^{-3})*	δ^{56}Fe ± 2SE (‰) **	Fe conc. (ng m^{-3})*	δ^{56}Fe ± 2SE (‰)**	δ^{56}Fe ± 2SE (‰)
		Total		Total	Total
14-A	1.54 (1 %)	n.a.	1.07 (23 %)	−0.64±0.15 (−0.41±0.13)	n.a.
14-B	0.62 (3 %)	0.06±0.18 (0.09±0.16)	1.20 (29 %)	0.41±0.14 (0.31±0.12)	0.29±0.11
14-C	0.98 (1 %)	0.43±0.11 (0.42±0.08)	0.46 (36 %)	0.39±0.12 (0.31±0.10)	0.42±0.08
14-D	0.13 (8 %)	n.a.	0.46 (38 %)	n.a.	n.a.
14-E	0.91 (1 %)	0.28±0.10 (0.26±0.08)	0.78 (26 %)	0.02±0.15 (0.05±0.13)	0.16±0.09
14-F	1.11 (1 %)	0.36±0.15 (0.35±0.14)	0.35 (43 %)	0.17±0.15 (0.16±0.14)	0.32±0.12
14-G	2.31 (2 %)	0.37±0.26 (0.37±0.25)	1.75 (36 %)	0.43±0.10 (0.34±0.07)	0.39±0.15
14-H	4.58 (1 %)	0.18±0.11 (0.17±0.09)	0.72 (28 %)	n.a.	n.a.
14-I	0.29 (4 %)	0.05±0.32 (0.06±0.31)	< D.L.	n.a.	n.a.
14-J	1.30 (1 %)	0.09±0.14 (0.09±0.12)	< D.L.	n.a.	n.a.
14-K	2.72 (0.4 %)	0.07±0.11 (0.07±0.09)	< D.L.	n.a.	n.a.
14-L	0.45 (3 %)	0.31±0.14 (0.31±0.12)	0.54 (36 %)	0.43±0.17 (0.30±0.16)	0.37±0.11
14-M	2.10 (0.5 %)	0.09±0.10 (0.09±0.07)	< D.L.	n.a.	n.a.
14-N	4.15 (1 %)	0.07±0.29 (−0.04±0.28)	4.94 (20 %)	−1.45±0.23 (−1.17±0.22)	−0.76±0.18
14-O	27.16 (1 %)	−0.24±0.24 (−0.30±0.23)	14.63 (13 %)	−2.16±0.30 (−1.72±0.29)	−0.91±0.19

*Fe concentrations were calculated after subtraction of blank concentration. Fraction of Fe in blank filter to sample filter is shown in the parenthesis.

** δ^{56}Fe values before the correction of blank filter is shown in the parenthesis.

Table S6. The fraction (%) of each Fe species estimated by the linear combination fitting of XANES spectra. n.a.: not available due to small quantity of sample Fe or high filter blank.

No.	Coarse				Fine			
	Fe-containing aluminosilicates	Fe(III) hydroxide	Fe oxides	*R*	Fe-containing aluminosilicates	Fe(III) hydroxide	Fe oxides	*R*
13-a	59	41	0	*0.013*	34	66	0	*0.012*
13-b	55	45	0	*0.026*	43	57	0	*0.028*
13-c	21	79	0	*0.013*	20	80	0	*0.029*
13-d	42	58	0	*0.012*	32	68	0	*0.012*
13-e	66	34	0	*0.013*	52	48	0	*0.017*
14-A	37	63	0	*0.014*	42	58	0	*0.021*
14-B	77	23	0	*0.022*	33	67	0	*0.029*
14-C	40	60	0	*0.016*	36	64	0	*0.044*
14-D		n.a.				n.a.		
14-E	35	65	0	*0.011*	27	73	0	*0.028*
14-F	36	64	0	*0.015*	33	67	0	*0.029*
14-G	52	48	0	*0.040*	44	56	0	*0.028*
14-H	56	44	0	*0.008*	24	76	0	*0.017*
14-I	82	18	0	*0.011*		n.a.		
14-J	21	0	79	*0.013*		n.a.		
14-K	23	12	65	*0.015*		n.a.		
14-L	27	23	50	*0.014*		n.a.		
14-M	36	28	36	*0.022*		n.a.		
14-N	54	46	0	*0.020*	36	64	0	*0.019*
14-O	35	65	0	*0.018*	12	88	0	*0.054*

Table S7. Total and soluble Fe deposition flux of natural and combustion Fe.

	Total Fe deposition flux (nmol m^{-2} day^{-1})		Soluble Fe deposition flux (nmol m^{-2} day^{-1})	
	Natural Fe	Combustion Fe	Natural Fe	Combustion Fe
group I	291	15	2.9	1.4
II	27	0	0.2	0
III	32	0	0.4	0

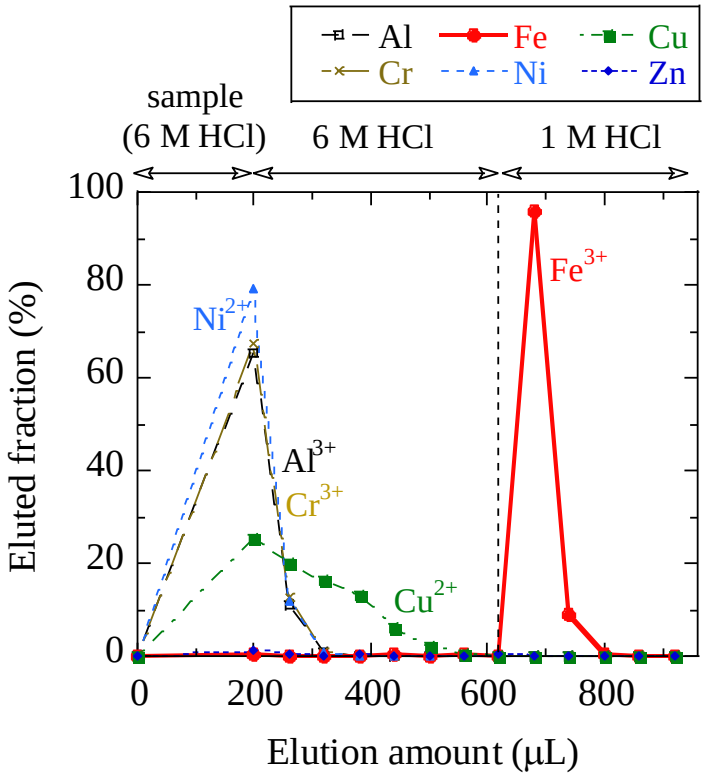

Figure S1. Elution curves of Al^{3+}, Cr^{3+}, Fe^{3+}, Ni^{2+}, and Cu^{2+} with the anion exchange resin.

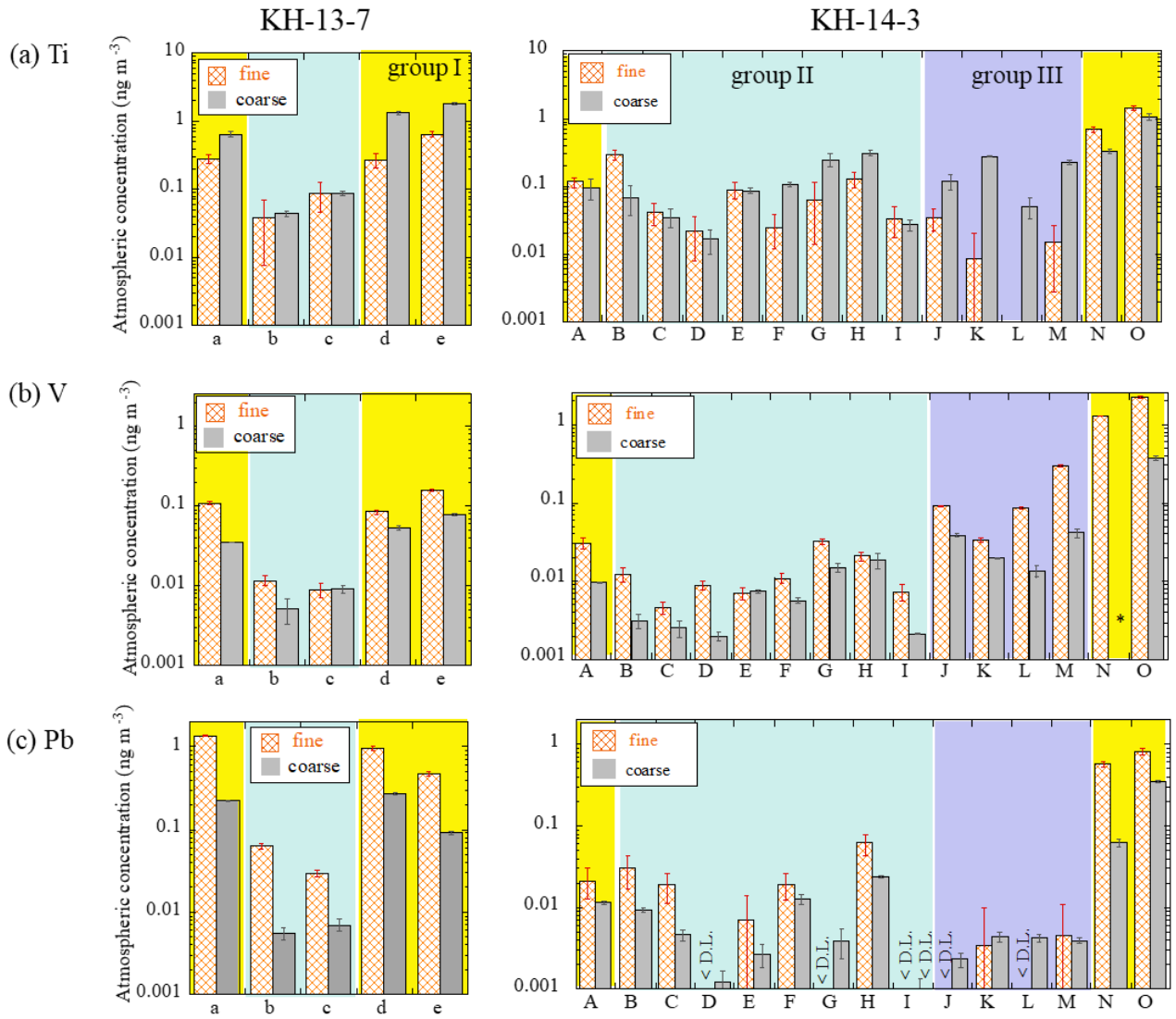

Figure S2. Atmospheric concentrations of (a) Ti, (b) V, and (c) Pb in size fractionated aerosols collected during KH-13-7 and KH-14-3 cruises. Errors are calculated from ICP-MS error and blank subtraction error. Yellow, blue, and purple areas indicate the group I (air masses from the Asian continent), II (air masses from the central and eastern Pacific), and III (air masses from the northern North Pacific), respectively. <D.L.: under detection limit due to higher concentrations in blank than samples.

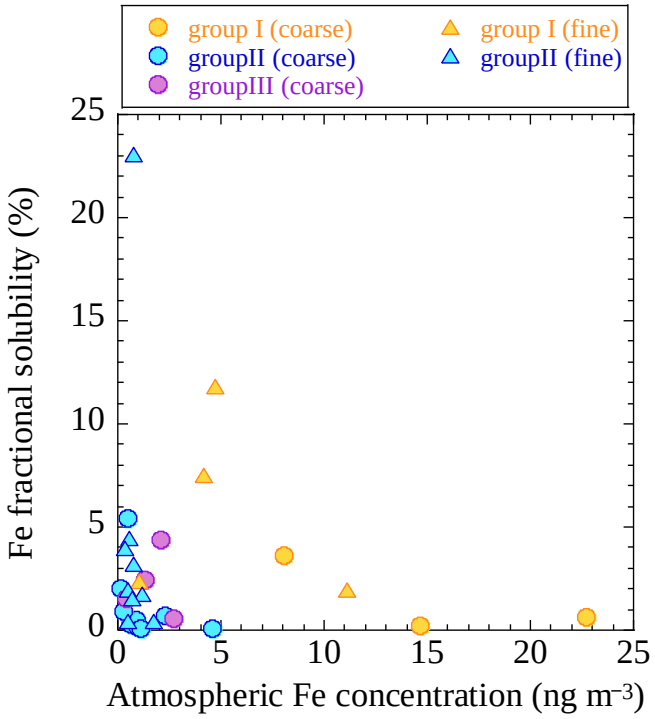

Figure S3. Scatter plot of atmospheric Fe concentration vs. Fe fractional solubility.

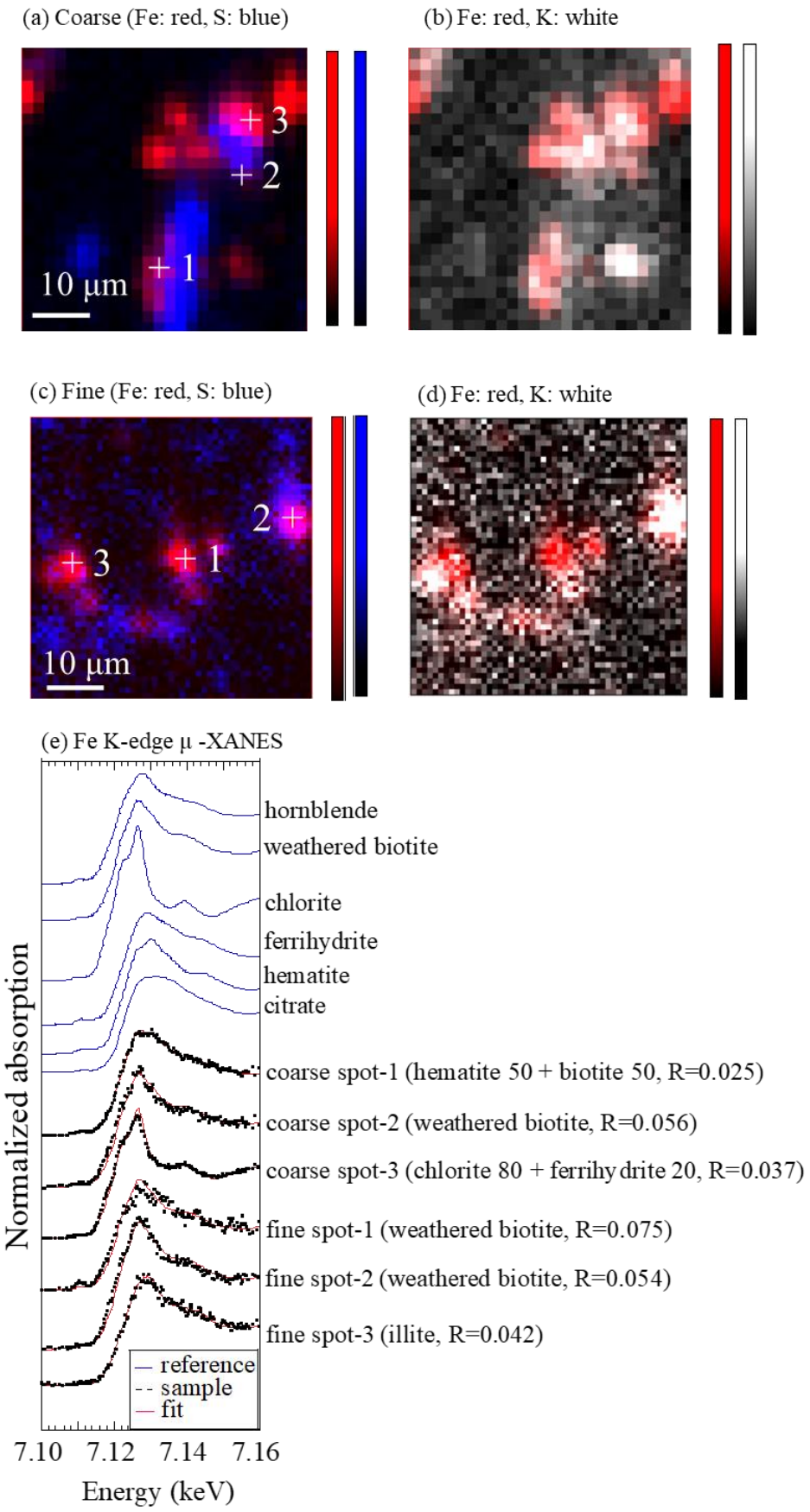

Figure S4. μ-XRF maps of Fe, S, and K in (a,b) coarse and (c,d) fine particles of 13-a. (e) μ-XANES spectra of the points in (a)-(d).

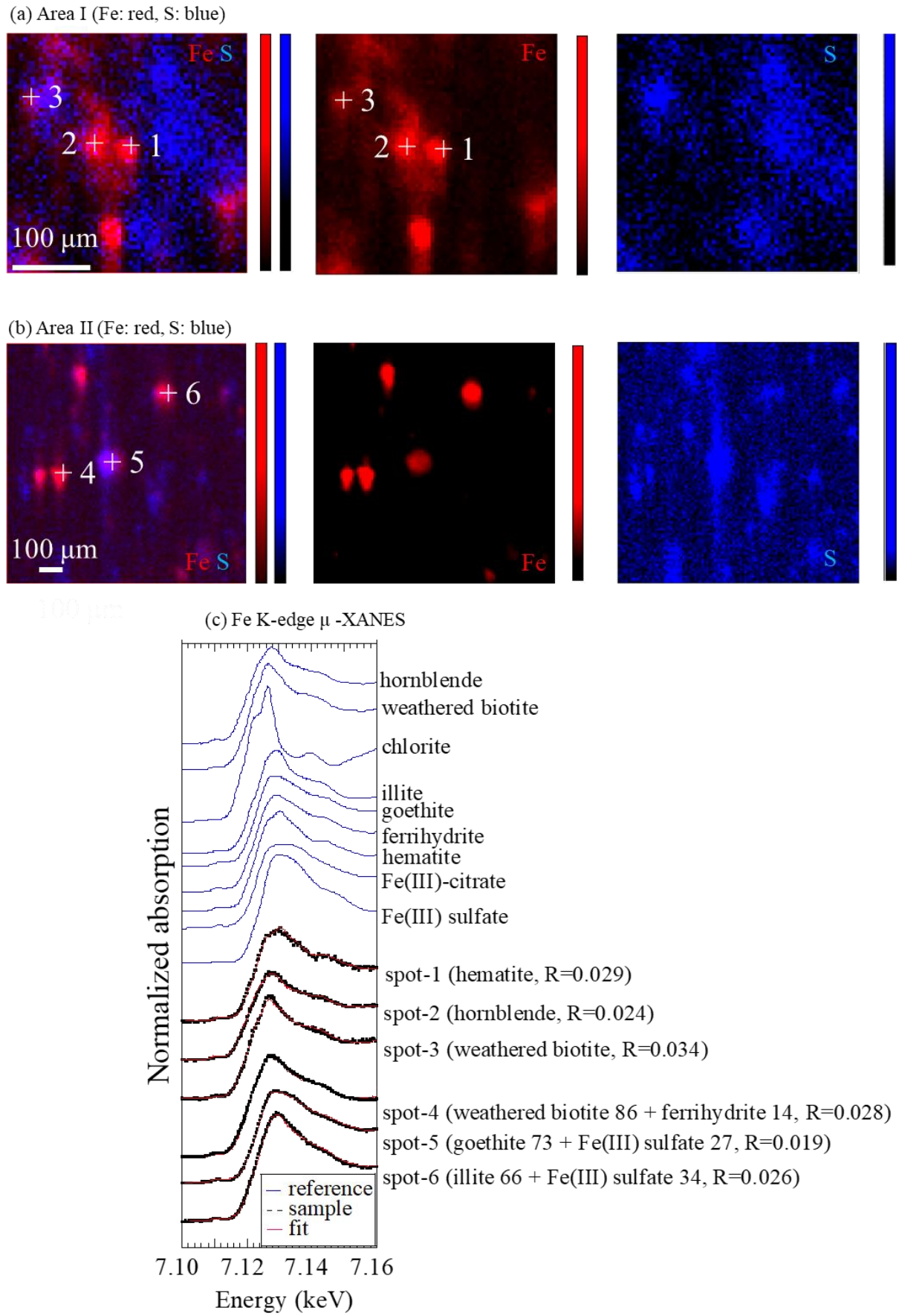

Figure S5. (a,b) µ-XRF maps of Fe and S in coarse particles of 13-c. (c) µ-XANES spectra of the points in (a-f).

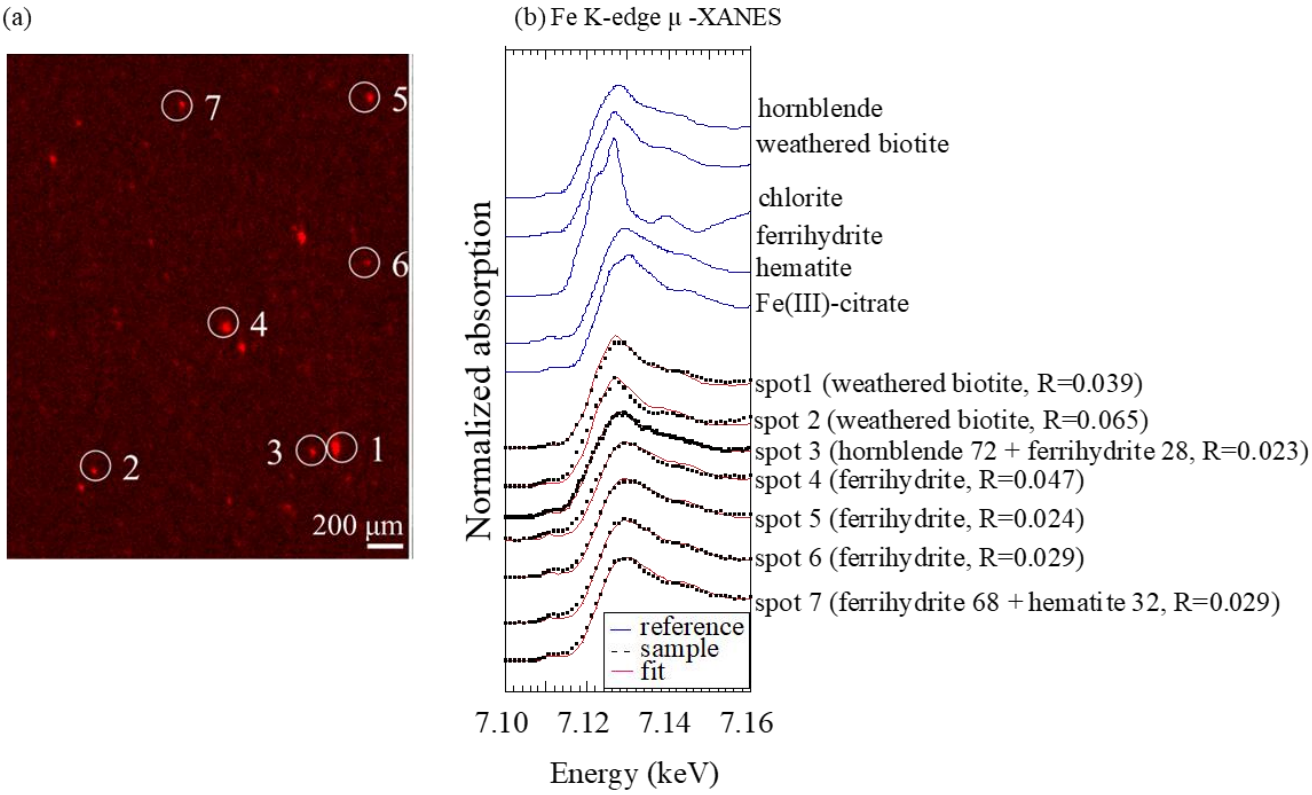

Figure S6. (a) μ-XRF maps of Fe in fine particles of 13-c. (b) μ-XANES spectra of the points in (a).

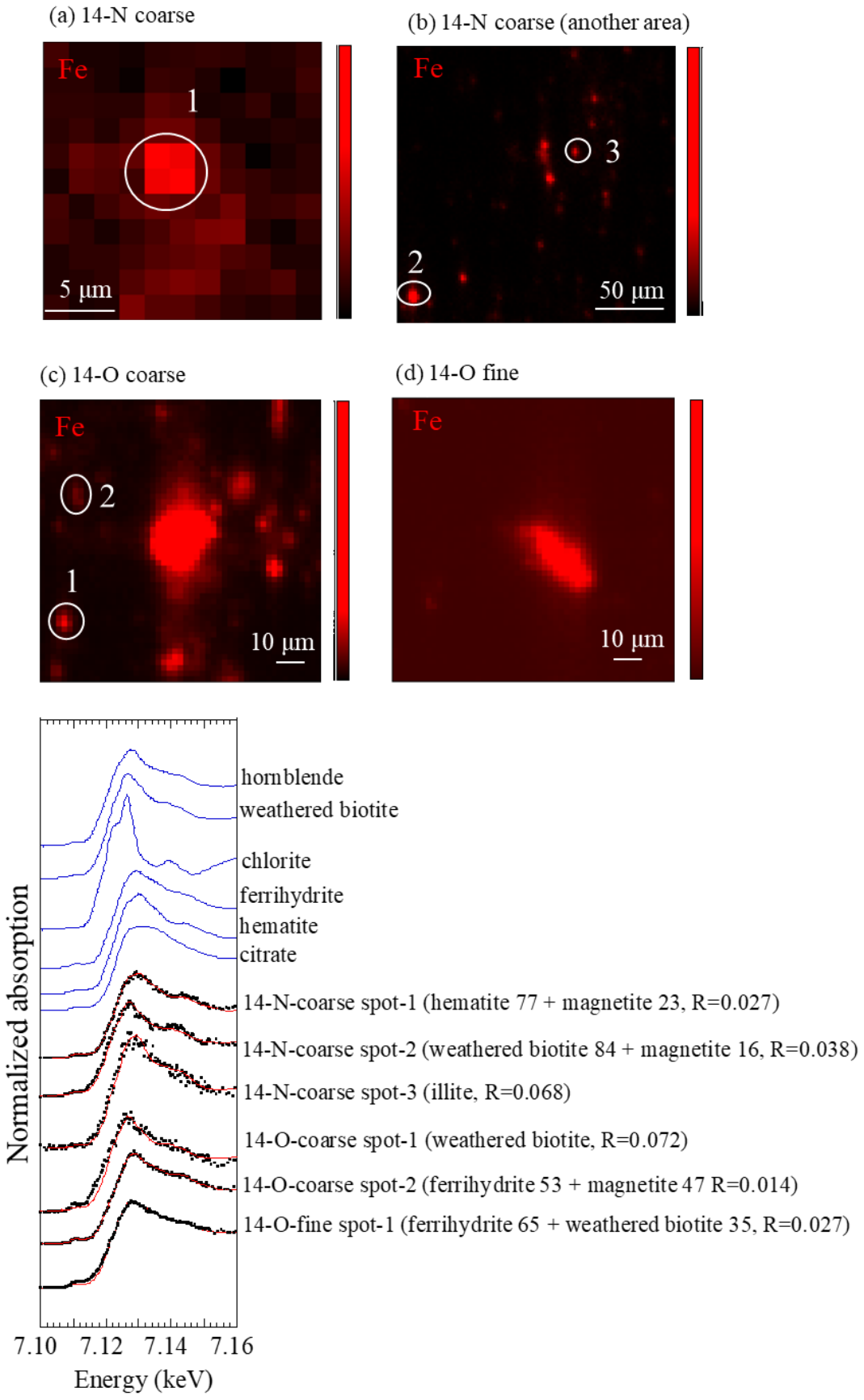

Figure S7. µ-XRF maps of Fe in (a, b) coarse particles of 14-N, (c) coarse particles of 14-O, and (d) fine particles of 14-O. (e) µ-XANES spectra of the points in (a-d).

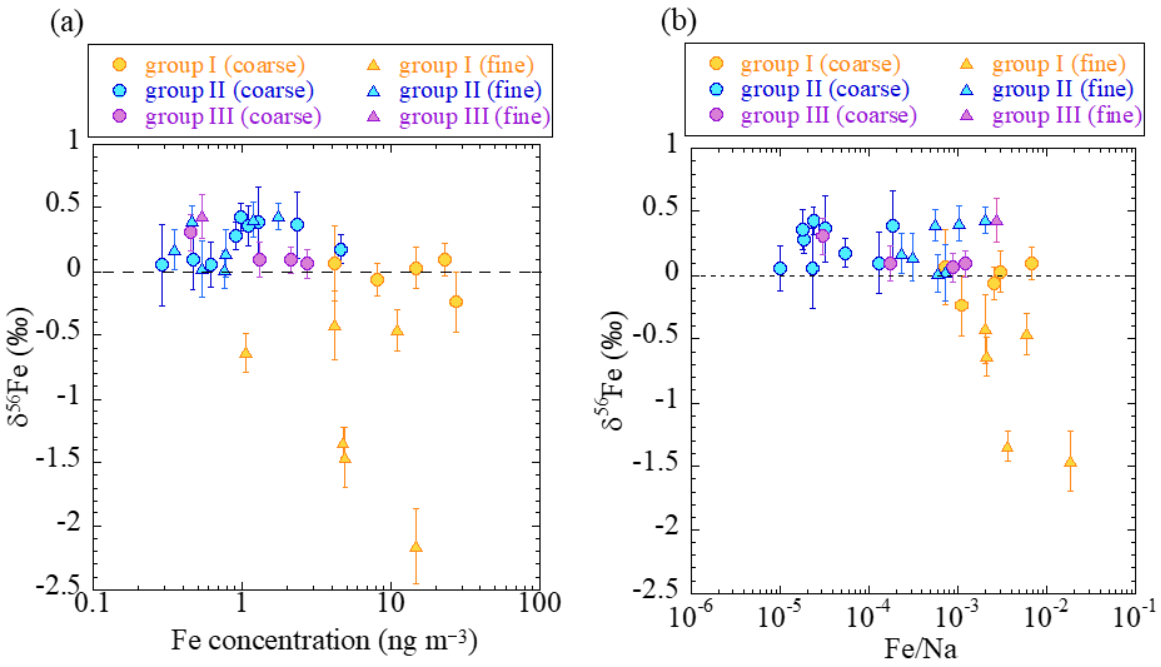

Figure S8. The relationship between (a) the atmospheric Fe concentration and δ^{56}Fe and (b) Fe/Na molar ratio and δ^{56}Fe. Na data were obtained from Sun et al. (2017). Note that the Fe/Na in surface seawater is 10^{-10}-10^{-8}.

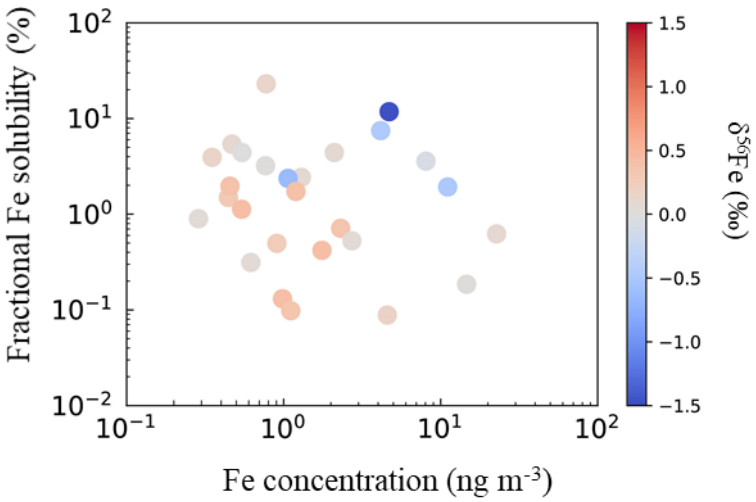

Figure S9. The relationship between the atmospheric Fe concentration and the fractional Fe solubility. The color scale indicates δ^{56}Fe.

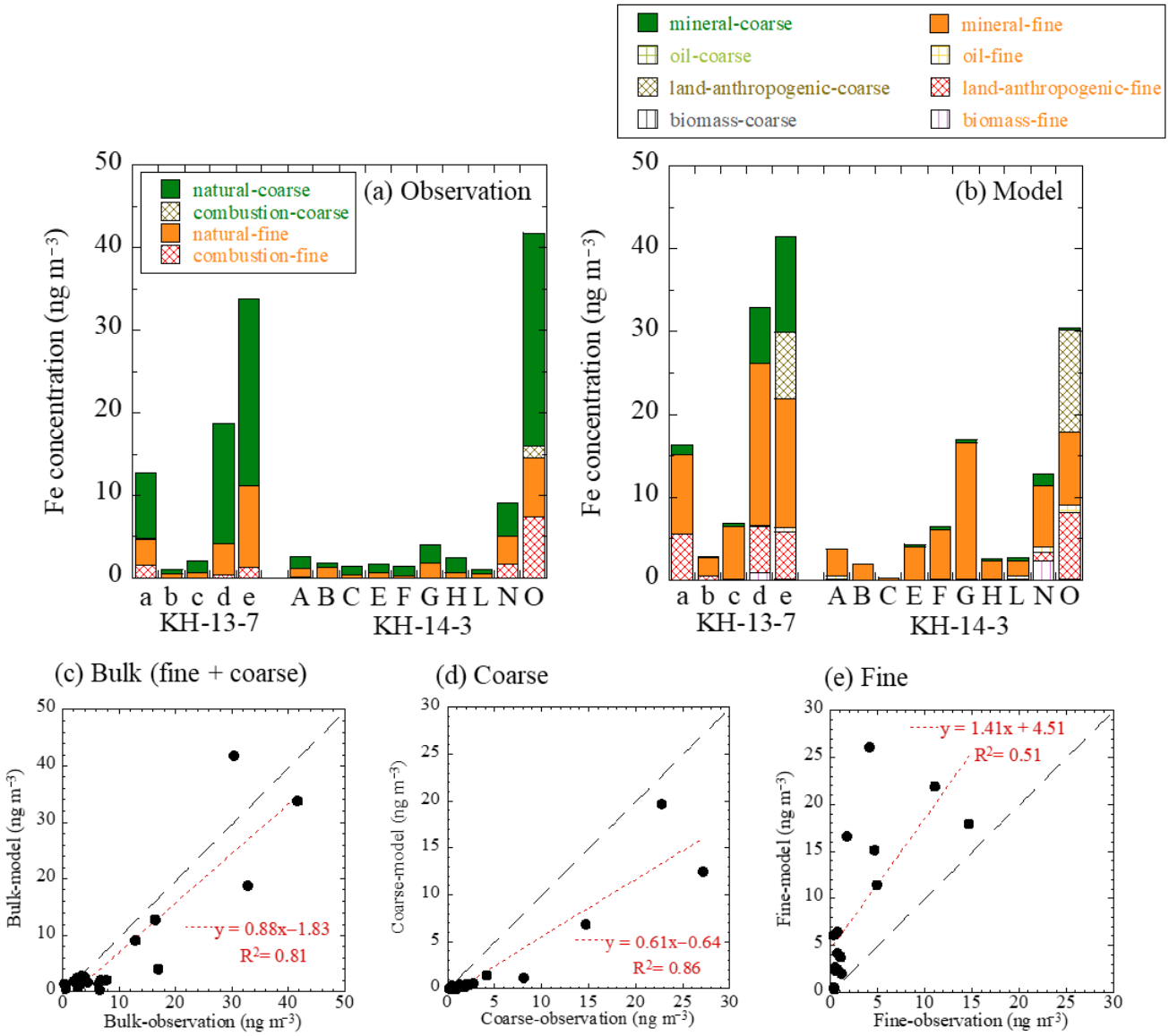

Figure S10. The Fe concentration from each source and size fraction calculated based on (d) the observation and (e) the IMPACT model; Comparison between the model-based estimation and the observation data for (a) the bulk (fine+coarse) Fe concentrations, (b) coarse Fe concentrations, (c) fine Fe concentrations.

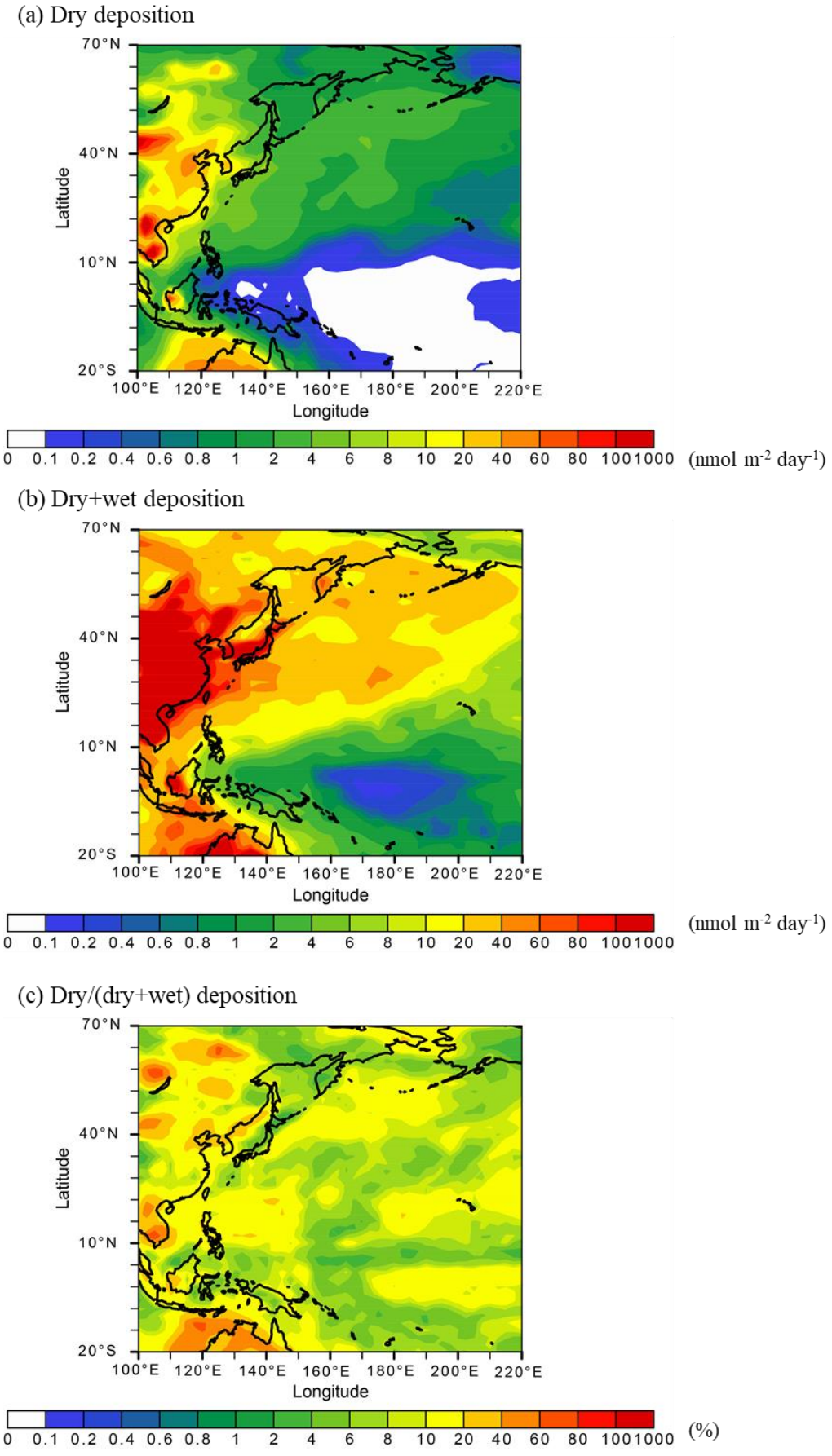

Figure S11. Deposition flux of soluble Fe by (a) dry and (b) dry+wet depositions estimated by the IMPACT model during the group I sampling period. (c) The fraction of dry deposition to the total deposition.